Multi-market Demand Response from pump-controlled open canal systems An economic MPC approach to pump scheduling.

Ties van der Heijden[a,b,c,*], Dorien Lugt[c], Ronald van Nooijen[a], Peter Palensky[b], Edo Abraham[a]

[a] *Water Resources Department, Faculty of Civil Engineering and Geosciences, TU Delft, Stevinweg 1, 2628 CN Delft, the Netherlands*
[b] *Electrical Sustainable Energy Department, Faculty of Electrical Engineering, Mathematics and Computer Science, TU Delft, Mekelweg 4, 2628 CD Delft, the Netherlands*
[c] *HKV Consultants, Informaticalaan 8, 2628 ZD Delft, the Netherlands*

Abstract

Participation in Demand Response (DR) has been explored for many large energy-using assets based on day ahead markets. However, little is known about the potential of DR for open canal systems. In this manuscript, we propose the use of multiple electricity spot markets to enable price-based DR for open canal systems in the Netherlands, where many large pumping stations are used for flood mitigation and control of groundwater levels. In the new strategy for pump-scheduling we combine the day ahead and intraday electricity markets to be used in a hierarchical receding horizon economic Model Predictive Control (MPC). A cost-potential analysis was performed for multiple market-strategies and the automatic Frequency Restoration Reserves (aFRR). We show new insights in the trade-off between CO_2 emissions and operating cost, and in the difference between the German and Dutch market. We observe that the German energy market is rewarding DR more than the Dutch equivalent, due to the higher renewable energy market penetration. The proposed multi-market strategy leads to a cost decrease of 10% and 16% in the Netherlands in 2017 and 2019, respectively. When applying German market scenarios, we found a cost saving potential of 46% and 50% in 2017 and 2019, respectively. The cost-saving potential for the aFRR-market was found to be up to 12% in the Netherlands and 28% in Germany, through a conservative analysis. The results suggest that the proposed control system, optimising costs over the day ahead, intraday and possibly the aFRR markets, is profitable compared to the current strategy in both the current and future electricity market.

Keywords: Demand Response, Electricity Markets, Open Canal Systems, Pump Scheduling, Water Resources Management.

1. Introduction

1.1. Demand response in the Netherlands

With climate change mitigation as a driving force, Renewable Energy Sources (RES) are becoming a larger part of the energy mix [1]. The Netherlands has passed a climate-law, in which the country commits to a 49% reduction of CO_2 emission by 2030 and 95% reduction by 2050 (compared to emission levels in 1990) [2]. Solar and wind energy are promising renewable energy sources, and are becoming more profitable due to technological advancements. While these generating-techniques are valuable for the energy transition, they bring some new challenges. One of these challenges is that the amount of energy generated at a certain time is as predictable as the weather. Big consumers will have to be more active when energy is available, and less when it isn't. The availability of energy is reflected in the price of flexible energy markets through

*Corresponding author
Email address: T.J.T.vanderHeijden-2@tudelft.nl (Ties van der Heijden)

scarcity of a product. This economic incentive to customers to shift energy use in time is known as Demand Response (DR) [3, 4].

Currently energy prices are correlated with sustainable energy production, as shown in Section 2.3. When wind power generation peaks unexpectedly, the price of energy decreases. This price decrease can even result in negative energy prices, since paying consumers can at times be less expensive than shutting down inflexible power plants. By consuming energy at the right time, money can be saved, or even earned by energy users; this gives DR a business case. DR can be enabled by participating on flexible energy markets, which give incentives to change energy usage through time-of-use pricing. Currently, these markets are changing to accommodate sustainable energy and flexibility in consumption [5].

Since the Dutch market currently has a low share of renewable energy, we take the German market as representative for a future scenario for the Dutch market. Germany's energy mix is increasingly dominated by wind and solar energy [6], which are the same sources the Dutch energy transition is moving towards [7]. In addition, the market structures are relatively similar in the two countries. Both countries make use of a Day Ahead Market (DAM) and Intraday Market (IDM). However, the balancing services are not open for public participation in Germany; this has already been realised in the Netherlands, where any Balance Responsible Party (BRP) can participate on the imbalance market [8].

1.2. Water management in the Dutch delta

The Netherlands is a low-lying country in the Rhine-Meuse delta, with the rivers Rhine, Meuse and Scheldt flowing through it. Since a large part of the country lies below mean sea level (MSL), managing water levels of local and national water ways is necessary. The water levels and type of management (fixed, flexible or dynamic water level) are decided locally by a waterboard for the smaller canals. Nationally the Dutch Ministry of Infrastructure and Water Management, Rijkswaterstaat (RWS), determines water levels typically based on agricultural needs, land-subsidence mitigation, shipping requirements and flood risk. Many of these canals are controlled by MPC, which still is an active topic of research in water resources management [9, 10, 11, 12, 13]. In these big canals and rivers, which are managed by RWS, there is generally room for more dynamic water levels. This range, in combination with the increasing presence of variable speed pumps, increases the flexibility in energy use within the water system [14]. Applying DR to the water system could reduce the CO_2 emission caused by the pumping stations' energy use, and would contribute to stabilising the Dutch electricity-grid. The Dutch water system has a power potential of 200 MW, and potential energy storage of 1700 MWh [15]. The system could be a valuable addition to the already contracted 300 MW [8] Automated Frequency Restoration Reserves (aFRR) capacity, which has recently been shown to be a suitable mechanism for DR participation [16].

1.3. Current status of DR applications

With rapid advances in intelligent electricity demand management systems and growth of aggregators, many more energy users are participating in DR [17, 18]. In fact, even power network expansion and renewable energy investment decisions have to explicitly consider a future with DR [19, 20]. Currently, some new assets that participate in DR include drinking water systems [21, 22, 23, 14, 24, 25] and HVAC systems [26, 27, 28, 29]. The DR strategies applied mostly involve a DAM [21, 23, 27, 28]. However, there is still variation in strategies applied. Some research the economic potential of the IDM [23], while others combine the DAM with the IDM to optimise cost [28]. Considering multiple market mechanisms can significantly improve economic efficiency of DR [30]. These types of spot market based DR is called time-of-use pricing and is part of the price-based DR class [4]. The potential cost- and emission-reduction through DR increases with renewable energy penetration [31]. DR strategies that include a short-term flexible energy market (like the IDM or market-based balancing services) [22, 28, 32, 33, 34] typically use mixed-integer formulations of the optimisation problem to indicate buy/sell scenarios [4]. However, in [35] a NLP is solved for to optimise dispatch on a microgrid. When applying DR, the Dutch or German market is hardly ever taken as case-study. These applications relate to energy markets in France [21, 24], the UK [22, 23, 14], Canada [26], the USA [27, 25, 33], Denmark [28] and South-Africa [34]. Other studies show the economic potential of the Frequency Restoration Reserves (FRR) for PV-battery systems [36], where a

rule-based control was simulated with Dutch market data. FRR potential was also explored for heat pumps in Germany [37] by simulating with a rule-based control system. In [38, 39], a stochastic MPC (MPC) was applied in a simulation of residential heating, energy storage and community integrated energy systems in order to explore technical feasibility and economic potential.

In this manuscript we propose a new pump scheduling strategy for water resources management that combines both the DAM and IDM, and consider scenarios with both the Dutch and German markets. We analyse market data from both countries, showing the effect of renewable energy market-penetration on the correlation between the carbon intensity (CI) of electricity and the DAM price (Section 2.3). Actual market data for the DAM, IDM and aFRR markets was used. The MPC formulated (Section 3.2) results in a Mixed Integer Quadratic Program (MIQP), which is solved and applied in a closed-loop simulation, using a receding horizon implementation. The proposed multi-market strategy is compared with a reference strategy, where energy use is minimised and energy is traded on the futures market for a monthly fixed price. Besides participation on spot markets (Section 4.2), we present an estimate of the economic potential for participating on the aFRR market, for which the potential of successful activation for downward regulation is analysed (Section 4.3).

2. Market- and balancing mechanisms

We evaluate the following mechanisms for DR purposes: the Day Ahead Market (DAM), Intraday market (IDM), futures market and aFRR market. The market mechanisms will be explained in the following section. Direct participation in the aFRR market is not simulated, but its potential is explored based on a post analysis using actual aFRR activation data (Section 4.3) and MPC simulations with participation on the DAM and IDM (Section 4.2).

The German market is taken as representative for a future Dutch market. The German RES mix is similar to the planned future mix in the Netherlands [6, 7], while the countries have a similar market structure, climate and socio-economically driven electricity consumption patterns.

2.1. Market mechanisms

On the DAM, energy is traded on a day-to-day basis with bids made for the following day. Consumers buy energy in hourly blocks, and have a responsibility to consume it within the period for which it is purchased. Every day at 12:00 CET, bids are collected by the market operator and the market is cleared at the price where supply meets demand. In the Netherlands, energy is traded on the APX-Endex, an energy-exchange.

The IDM is a continuous market where participants trade quarterly, 30-minute or hourly blocks of energy throughout the day, up to 5 minutes before delivery. On the IDM, buy- and sell-orders are matched individually, leading to different prices for all contracts. In this manuscript, the volume-weighted price over the three hours before delivery (ID3-price) is used. The IDM allows a user to buy and sell energy throughout the day, correcting their day ahead plan while preventing them from causing imbalance. The IDM is seen as the market containing the highest potential to trade renewable energy in the future [40].

Both the DAM and the IDM incentivise participants to adjust energy planning for favourable prices that reflect scarcity of supply and marginal cost of production. Minimising operational cost of energy will lead to a shift in energy use when prices change; a mechanisms known as price-based DR [4]. Figure 1 shows the 2-Dimensional Kernel Density Estimate (KDE) of the Dutch (Figure 1a) and German (Figure 1b) DAM and IDM price over recent years. The price difference between the two markets causes change in scheduling energy use or production. The distribution of the Dutch prices is varying more over the years than the distribution of the German prices. A possible explanation is the maturity of the markets: the German market is more mature in volume and therefore possibly more stable.

The futures market is where long-term or base-load products can be traded. Energy users trade here to reduce their risks, while producers trade here to ensure future sales and decrease vulnerability for electricity price decreases [41]. The market does not reward flexibility in energy use, since the price is fixed. Currently RWS trades on this market, buying futures contracts that guarantee a base-load over a longer period of time. We will compare the current futures market strategy with a multi-market strategy, where energy is bought on both the DAM and IDM.

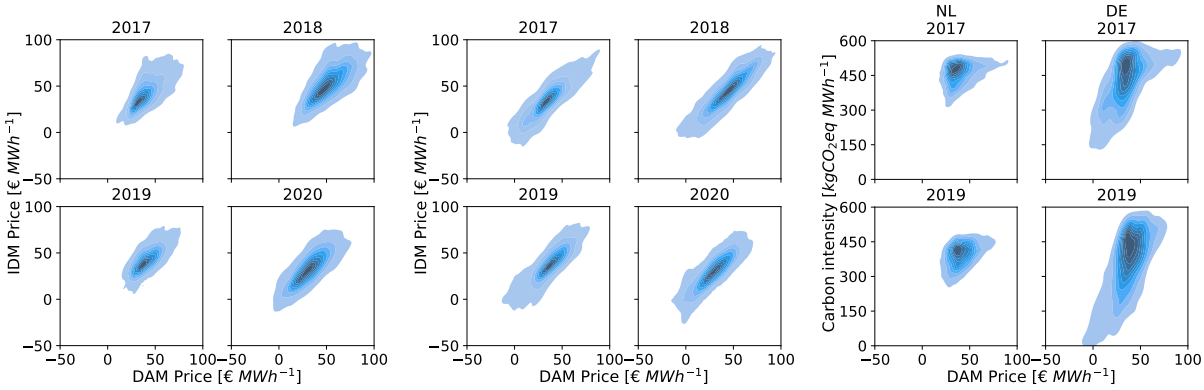

(a) Dutch spotmarket data (b) German spotmarket data (c) Estimated CI over DAM price.

Figure 1: 2-Dimensional KDE of the Dutch (a) and German (b) DAM and IDM price, and the estimated CI over the DAM price (c).

2.2. Grid balancing mechanisms

The Dutch Transmission System Operator (TSO), TenneT, is responsible for balancing the grid. It does so by employing balancing mechanisms, like the imbalance market. Because large volumes of energy cannot yet be stored with economic efficiency, power supply and demand have to be matched continuously. Imbalance on the grid can negatively affect power quality or can eventually result in damage to the infrastructure itself. TenneT balances the grid using back-up (emergency) production capacity or asking producers to reduce production. Another option is to ask large consumers to in- or decrease consumption, which is currently being applied to greenhouses, hospitals and small industries. Demand-side balancing of the grid is mostly implemented using automated control, powered by a near-real-time feed of the imbalance and energy price [42]

The aFRR is a reserve capacity market used to restore the grid frequency automatically when deviations from 50 Hz occur. On this market, BRP's can bid (with a minimum bid-size of 1 MW) for upward regulation or downward regulation. This is done per 15 minute blocks, and the BRP gets a 15-minute notice before activation. This market would be feasible for a pumping station to participate in, due to the 15-minute ramp-up time. The aFRR does constrain its participants to a minimum bid of 1 MW, a constraint that can be avoided by partnering with an aggregator that combines multiple small bids into larger bids. Figure 2 shows the probability of occurrence of downward activation on the aFRR market for certain downward regulating prices and activation sequence lengths. The German market shows a higher profit potential for downward regulating services. Interestingly, the data shows small differences over the years, indicating that the increase in renewable energy generation does not increase the demand for downward regulation through the aFRR. The IDM, which is more easily accessible to BRPs, might be providing the necessary balancing while allowing BRPs to mitigate risks of trading for disadvantageous prices.

2.3. Carbon intensity of electricity on the grid

Optimising on energy costs can lead to a decrease in emitted CO_2 [31] due to the correlation between sustainable energy production and energy price. Two national markets are evaluated: the Dutch and the German market. The Netherlands has a low share of RES, while the German energy mix contains a larger share. The merit-order effect, where RES with low marginal costs of electricity are activated before more polluting sources with higher marginal costs, increases the correlation between CI and energy price in the German market.

Due to incorrect ENTSO-E Electricity generation by source time series, a CI time series of the grid was not easily estimated. First, historic solar and wind generation time series are calculated using 'Renewables.Ninja' capacity factor time series [43, 44] for both the Netherlands and Germany. The yearly installed capacities [45,

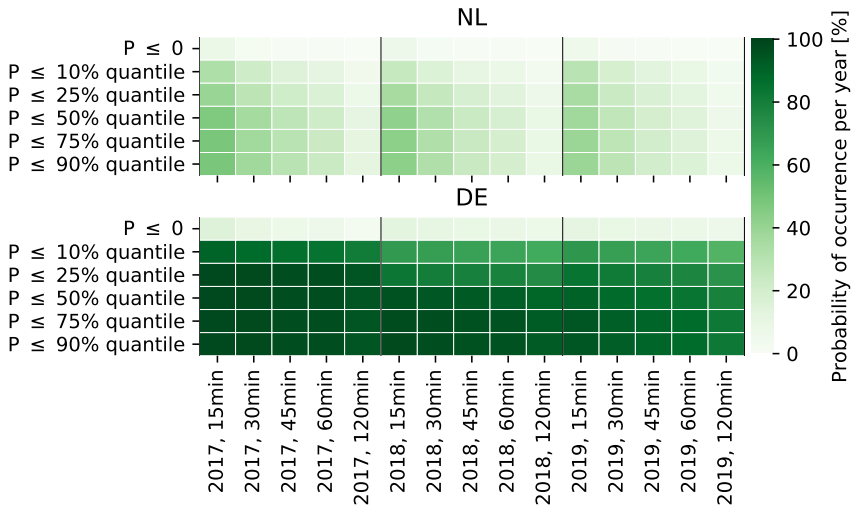

Figure 2: Probability of occurrence of downward activation through the aFRR market. The figure shows the percentage of time at which downward activation occurred in color, the year and the length of the activation sequence (15min, 30min, 45min, 60min) on the x-axis. On the y-axis is the downward regulating price at ≤ 0, or less than a quantile value of the DAM prices that year.

46] were linearly interpolated over time in order to have time series of installed capacity. The resulting renewable energy generation time series are corrected with the yearly produced renewable energy volumes [45, 47] by scaling the time series to match the reported yearly produced generation volumes. For every hour, the emitted carbon from renewables is calculated based on the CI of electricity produced by renewable sources [48, 49]. The total emitted carbon per year is then calculated using the load and the reported yearly averaged CI [45, 50]. The yearly emitted carbon from renewables is then calculated, and subtracted from the total emitted carbon. Consequently, the emitted carbon from non-renewable sources remains. The yearly average 'rest' CI is calculated using the previously calculated non-renewable carbon emission, and the amount of load not supplied by renewables. The yearly averaged CI is then linearly interpolated over the intermittent dates to a 'rest' CI time series. The CI time series of all generation is consequently calculated by dividing the emitted carbon at each hour by the load.

Figure 1c shows the estimated CI of the two national grids plotted over the DAM prices for 2017 and 2019. For both considered markets, a correlation can be seen between the DAM price and the CI of energy. In Germany, the spread of the CI is larger than in the Netherlands. The Netherlands contains the relatively efficient coal- and gas-fired power plants, while Germany still uses brown-coal plants to produce electricity to some degree [51]. Also, Germany has a larger share of renewables which at some times can even fulfill all the electricity demand, leading to a strong correlation between DAM prices and CI.

3. Case Study Area for Demand Response: modelling the water system and DR participation

We apply the multi-market strategy to the water system of the Noordzeekanaal–Amsterdam-Rijnkanaal (NZK-ARK). The NZK-ARK is a complex open canal system, containing multiple undershot gates and a pumping station at IJmuiden to enable the discharge of water into the North Sea, whether the sea water level is high or low. The system receives water from four waterboards (local water authorities) who discharge excess rainwater into the system, which is then pumped or sluiced out to the North Sea. The NZK-ARK is also used for ship traffic, which imposes a strict lower and upper bound on the water level. These constraints prevent cargo-ships from hitting the bottom and to make sure ships can pass bridges.

At IJmuiden, the gates are opened at a difference in water level of 16cm, and closed at 12cm [52]. This difference in pressure is needed to overcome the difference in density of fresh and salt water together with

Pump	RPM/Discharge	Q-dH relationship [m^3/s], [m]	P-dH relationship [kWh], [m]
1&3	n = 64.3 rpm	$Q = -5.4174 \cdot dH + 44.93$	$P = 208.08 \cdot dH + 536.85$
2&4	n = 64.3 rpm	$Q = -5.4174 \cdot dH + 44.93$	$P = 208.02 \cdot dH + 536.85$
	n = 48.2 rpm	$Q = -6.4977 \cdot dH + 33.149$	$P = 192.36 \cdot dH + 217.26$
	n = 50 m^3/s	$Q = -1.9822 \cdot dH^2 + 1.9726 \cdot dH + 44.93$	$P = 443.91 \cdot dH + 476.3$
5&6	n = 40 m^3/s	$Q = -1.8544 \cdot dH^2 + 7.774 \cdot dH + 44.93$	$P = 379.09 \cdot dH + 373.18$
	n = 30 m^3/s	$Q = -7.1021 \cdot dH + 48.164$	$P = 282.97 \cdot dH + 417.32$

Table 1: Pump power and discharge curves [53]

internal friction. The gate is controlled automatically and has a maximum discharge of 500 m^3/s. This maximum discharge is maintained to ensure stability of the bed of the gate-complex. The pumping station in IJmuiden contains six pumps, with a combined maximum power consumption of around 4.9 MW. The pumps can only pump up to a certain water level difference, when the height differential is too high they will automatically shut down. Currently, pumping station IJmuiden is controlled through an MPC that minimises energy use while energy is bought on the futures market. In this MPC, the prediction horizon is 24 hours, and the water level is kept between -0.3m+NAP and -0.5m+NAP. For DAM participation, a prediction horizon of at least 36 hours is necessary to submit a full bid before market closure. In this research, a prediction horizon of 48 hours was applied to investigate the economic potential of DR for the water system.

Table 1 contains the Q-dH (discharge - pump height), and P-dH (power - pump height) relationships for each of the six pumps. To solve a single MPC problem for the whole pumping station, we formulate a single simplified Q-dH curve by using the separate Q-dH curves for the pumping station as described in Section 3.3. We used the P-dH curves in Table 1 to formulate a single equivalent PQH-curve for the pumping station, which describes pump power consumption as function of pump discharge and pump height. The novel method we have applied to formulate the representative PQH-curve is described in Section 3.3.

3.1. Water system modelling

In the MPC's internal model, we represent the canals of the system as simple storage components: i.e. a bucket with a fixed surface area that is used to describe the relationship between storage and water level in the canals. A similar model is currently being applied in the control system of the NZK-ARK [54]. The incoming fluxes are the waterboard discharge and the discharge measured in Maarssen, the outgoing fluxes are the pump- and gate-discharge into the North Sea. Delay or routing is not taken into account and is assumed negligible due to the low flow speeds taking place in the system, leading to low friction.

The gate-complex in IJmuiden has 7 square tubes, which contract in the middle to regulate discharge. They are 5.9m wide and the height of the "throat" of a tube is 4.8m above the bottom. It has a maximum discharge of 500 m^3/s, imposed for the stability of the bed and structure [55]. There are seven square tubes that can be (partially) closed to regulate the flow. The equation describing its behaviour is [56]

$$Q_{max}[t] = n \cdot \alpha \cdot B \cdot h_k \cdot \sqrt{2 \cdot g \cdot (h_i[t] - h_o[t])}, \tag{1}$$

with $Q_{max}[t]$ as the maximum discharge at time t, n the amount of tubes, α the contraction coefficient, B the width of a tube, h_k the height of the center of the tube, g the gravitational constant, $h_i[t]$ the water level of the NZK at time t and $h_o[t]$ the water level of the North Sea at time t.

The pumping station in IJmuiden consists of 6 pumps: two fixed-speed pumps, two pumps with two settings, and two variable speed pumps. The combined maximum discharge is 260 m^3/s. The pumping station is modelled by simplifying it to a single pump. Pump-characteristics are combined to estimate the equivalent characteristics. Since there are 6 pumps present in the pumping station, with different properties, multiple Q-dH curves and power-curves are used to describe the station. Table 1 shows these curves for all three types of pumps present in the station. To account for the effect of the wind on the water level, wind data of the KNMI station in IJmuiden has been used to estimate the water level change.

We solve the MPC problem to determine the optimal control settings for multiple gates and the pumping station at IJmuiden. The gates and pumping stations are represented using a single gate and single pump with an aggregated Q-dH and QPH-relationship.

3.2. Economic MPC formulation with multiple markets

We propose a two-stage MPC for participating in DR through the use of both the DAM and IDM. The MPC involves buying energy on the DAM for 24 hours and then iteratively deciding on how to deviate from this plan based on rewards on the IDM. As such it solves two optimisation problems in a receding horizon fashion subject to physical constraints for the water system. IDM trading occurs with a shrinking horizon stretching until the next DAM-bid is made. The two-stage MPC applying the multi-market strategy is compared to a reference scenario without DR, where energy use is minimised and energy is purchased for a fixed price on the futures market.

Two objective functions belong to the proposed multi-market strategies, where an objective function is formulated for both the day ahead planning and the intraday trading phase. A third objective function is applied in the reference strategy without DR. For the DAM planning, an indication of the hourly prices of the next day is needed. In this research we have assumed perfect knowledge, where we minimise costs based on the observed prices. In future work we will include probabilistic forecasts of the DAM and IDM price, for example by generating price scenarios and apply tree-based MPC [57]. The economic objective function for DAM bidding is

$$\min J_1 := \underbrace{\sum_{t=0}^{N} (P[t] \cdot \frac{\Delta \mathrm{t}}{\gamma_c} \cdot \ c_{da}[t])}_{\text{day ahead bid}}, \tag{2}$$

where

$$P[t] := a_p \cdot \ Q_p[t]^2 + b_p \cdot \ dH_p[t]^2 \cdot \ Q_p[t] + c_p \cdot \ Q_p[t] \cdot \ dH_p[t], \tag{3}$$

$$dH_p[t] := h_{ns}[t-1] - h[t-1] - dh_w[t-1], \tag{4}$$

and $P[t]$ is the pumping power in kW, Δt the timestep size in seconds, γ_c is used to convert kWs to MWh, c_{da} is the DAM price in [€/MWh], t is the timestep index, N is the prediction horizon length in number of timesteps, a_p, b_p, c_p are the fitted parameters for the pump power-curve, dh_w and h_{ns} stand for the increment of water level at the gates and pumps due to wind effects and the water level of the North Sea, respectively.

The IDM allows for extra flexibility since the market allows trading up to 5 minutes before consumption. This makes the IDM a valuable addition to the DAM, since unforeseen external disturbances on the water system could be made up for or exploited by trading the energy surpluses or deficits during the day. We used the ID3 IDM price, which is the volume weighted price of a certain delivery hour in a 3 hour window preceding delivery. The economic objective function used for IDM trading is

$$\min J_2 := \underbrace{\sum_{t=0}^{t_d} ((P[t] \cdot \frac{\Delta \mathrm{t}}{\gamma_c} - E_{plan}[t]) \cdot \ c_{id}[t])}_{\text{intraday trading}} + \underbrace{\sum_{t=t_d}^{N} (P[t] \cdot \ \frac{\Delta \mathrm{t}}{\gamma_c} \cdot \ c_{da}[t])}_{\text{day ahead bid preparation}}, \tag{5}$$

where $E_{plan}[t]$ the energy bought on the DAM for time t, c_{id} the IDM price, t_d the timestep at which the next DAM bid starts. The first term allows for IDM trading, where deviations from the DAM bid are allowed at IDM prices for the time a DAM bid has been made (until t_d). The second term prepares the next DAM bid (starting at t_d) where costs are minimised based on DAM prices for the remaining length of the prediction horizon (N).

We compare the proposed multi-market strategy with a reference strategy where energy is bought on the futures market for a monthly fixed price. In the reference strategy, the objective is to minimise energy

use of pumping, resembling the current strategy employed by RWS. The objective function for the reference scenario is

$$\min J_3 := \underbrace{\sum_{t=0}^{N} P[t] \cdot \frac{\Delta \mathrm{t}}{\gamma_c}}_{\text{energy use minimisation}}, \tag{6}$$

with $P[t]$, Δt, N and γ_c as defined above.

3.3. Water system constraints

There are various safety and performance constraints (eg. water level and discharge limits) that need to be dealt with explicitly by the model predictive controller.

Although the lower bound on water level is a strict constraint for transport purposes, it may be tolerable to marginally violate the upper bound for small time periods. Therefore, the upper bound of the water level constraint was relaxed with a slack variable, and a penalty for exceeding the upper bound was introduced in the objective function. This was done to improve robustness of the computational model, so the problem would not become infeasible in high-water situations but rather the small violations could be analysed a posteriori. The lower and upper water-level bound constraints are reformulated as

$$h[t] \geq h_{min}, \tag{7}$$

$$h[t] \leq h_{max} + s[t], \tag{8}$$

where the discretised slack variable $s[t]$ represents the constraint violations on the maximum water height h_{max} at timestep t. The upper bound relaxation is implemented as a lazy constraint, meaning it is only active when a constraint violation on the un-relaxed upper-bound occurs. The penalty function

$$f_1(\cdot) := \gamma_s \cdot \sum_{t=0}^{N} s[t]. \tag{9}$$

sums up the discrete slack variables (i.e. bound violations per timestep), which automatically minimises the time and magnitude of constraint violations. This is added to the economic cost in the MPC optimisation problem in Equation (4), Equation (5) and Equation (6). The constant γ_s was chosen a posteriori to be sufficiently high, in order to prevent compromises between energy costs and constraint violation.

The water level associated with a given storage is calculated using a mass balance: the difference in water level is equal to the net flux that leaves or enters the body, divided by the surface area of the wetted water body. Because water is assumed in-compressible, a mass balance can be expressed in terms of volume

$$h[t] = h[t-1] + \frac{\Delta \mathrm{t}}{A_{nzk}} * (Q_{in}[t-1] - Q_g[t-1] - Q_p[t-1]), \tag{10}$$

where $h[t]$ is the water level of the NZK-ARK at time t in m+NAP, Δt the timestep size in seconds, A_{nzk} the surface area of the NZK-ARK in m^2, $Q_{in}[t]$ the incoming discharge of the ARK (the discharge in Maarssen, water coming from the Oranjesluizen and pumped discharge from the waterboards) at time t in m^3/s, $Q_g[t]$ the discharge from the gates, and $Q_p[t]$ the discharge of the pumping station in IJmuiden at time t in m^3/s.

The gates can only discharge when the water level of the North Sea is lower than the water level of NZK-ARK, and the pumping station can only discharge when the water level of the North Sea is higher than the water level of the NZK-ARK. To ensure this, a big-M formulation is applied. Two binary variables, z_g and z_p are introduced, which indicate the possibility of using the gates or pumping station, respectively

$$h[t] - h_{ns}[t] - dH_{g,min} + (1 - z_g[t]) \cdot M_g \geq 0, \tag{11}$$

$$h[t] - h_{ns}[t] - dH_{g,min} - z_g[t] \cdot M_g \leq 0, \tag{12}$$

$$h_{ns}[t] - h[t] - dH_{p,min} + (1 - z_p[t]) \cdot M_p \geq 0, \tag{13}$$

$$h_{ns}[t] - h[t] - dH_{p,min} - z_p[t] \cdot M_p \leq 0, \tag{14}$$

where h_{ns} is the water level of the North Sea, $dH_{g,min}$ the minimum water level difference needed to discharge with the gate, and $dH_{p,min}$ the minimum water level difference needed to discharge with the pumps. The big-M constants, M_g and M_p were chosen sufficiently large.

The discharge of the gate is a decision variable in the optimisation problem. The gate discharge relationship in Equation (1) was simplified through piecewise linearisation (PL). The feasible gate discharge region and the PL can be see in Figure 3a. The majority of the feasible region is constrained by the upper bound on gate discharge, rather than the Q-dH relationship. The gate discharge is bound to [0, 500], and the upper bound on gate discharge is multiplied with the binary variable z_g that indicates gate discharge possibilities

$$Q_g[t] \leq (a_g \cdot dH_g[t]) + b_g[t]) \cdot z_g[t], \tag{15}$$

$$dH_g[t] := h[t] - h_{ns}[t], \tag{16}$$

with $Q_g[t]$ being the gate discharge at time t, and a_g and b_g being the fitted parameters for the PL of the upper bound on gate discharge.

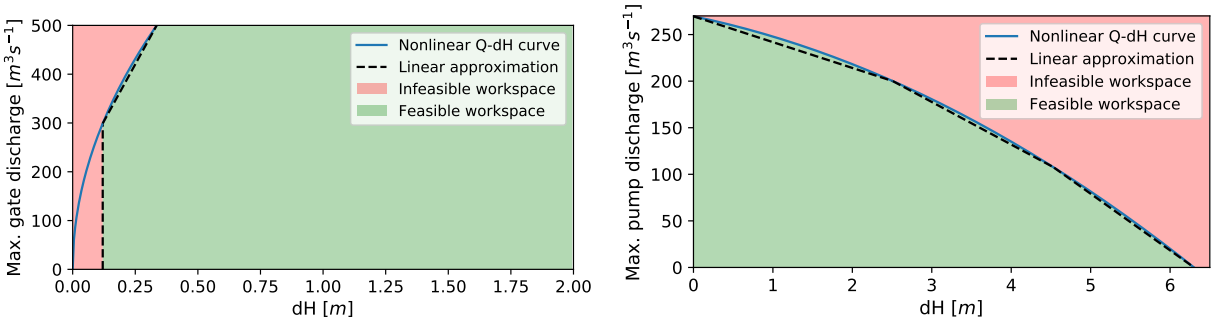

(a) Q-dH relationship for the undershot gates.

(b) Q-dH relationship for the pumping station.

Figure 3: Feasible (green) and infeasible (red) region for the discharge from undershot gates (a) and the pumping station (b) in IJmuiden.

Pump discharge capacity given a certain pump height is generally described through the use of Q-dH curves, where the (maximum) discharge is a function of the pump height. In the case of IJmuiden, six pumps are present with different curves describing their maximum discharge as a function of pump height. In order to represent the pumping station as one big pump, the different Q-dH relationships of the 6 separate pumps found in Table 1 are aggregated. For a given water level difference dH_p, the maximum discharge of the six pumps combined is equal to the sum of the maximum discharges for the individual pumps

$$Q_p[t] \leq \sum_{i=1}^{6} Q_i(dH_p[t]), \tag{17}$$

$$dH_p[t] := h_{ns}[t] - h[t], \tag{18}$$

with $Q_p[t]$ being combined pump discharge for the pumping station, and Q_i the maximum discharge of pump i as function of the pump-height dH_p. The resulting quadratic description of the Q-dH relationship is approximated through PL, as shown in Figure 3b. The PL is applied as an upper bound constraint on pump discharge, where the total upper bound is multiplied with the binary variable z_p indicating pump discharge possibilities

$$Q_p[t] \leq (a_p[i] \cdot (h_{ns}[t] - h[t]) + b_p[i]) \cdot z_p[t] \text{ for } i \in (1, 2, 3), \tag{19}$$

with a_g and b_p representing the coefficients of the PL-approximation of the Q-dH relationship.

In practice, the power consumption of the pump station can vary, depending on multiple operating conditions like pump configuration, pump height and discharge. The derived Q-dH curve for the pumping station acts as upper bound constraint for discharge at a given head difference. However, when deciding a combination of (Q_p, dH_p), energy use should be considered. Although the energy use of the pumping station could be directly represented using binary variables to act as an on/off switch for every separate pump, this results in computationally infeasible large scale mixed-integer nonlinear programs [58]. A novel approach that is in-between was applied. In the approach, the pumping station was represented using a single aggregate power curve so that the resulting MPC optimisation problem is a non-convex MIQP. Discretising the feasible domain in Equation (17) results in solving a MIQP for each aggregate (Q_p, dH_p) combination, optimising individual pump combinations and their respective discharges in order to minimise pump power consumption. Gurobi [59] was used to solve the MIQP. The function

$$P[t] := a_p \cdot Q_p[t]^2 + b_p \cdot dH_p[t]^2 \cdot Q + c_p \cdot dH_p[t] \cdot Q_p[t] \tag{20}$$

was fitted through these points, where parameters of the least squares fit were found to be: $a_p = 0.033$, $b_p = 0.061$ and $c_p = 11.306$. This equivalent power curve was used in the objective function as described in Equation (3).

3.4. MPC optimisation problem

To calculate optimal control settings for pumps and gates, the model is expressed as a non-convex Mixed Integer Quadratic Problem, to be solved with Gurobi [59] with the NonConvex parameter set to 2, the MIPGap set to 2%, the Absolute MIPGap set to €1,-, and the time limit set to 15min. Figure 4 shows the percentage that combined termination conditions occurred for the individual optimisation problems. The figure shows that the majority of optimisation problems is solved at the termination conditions, rather than cut-off at the time limit.

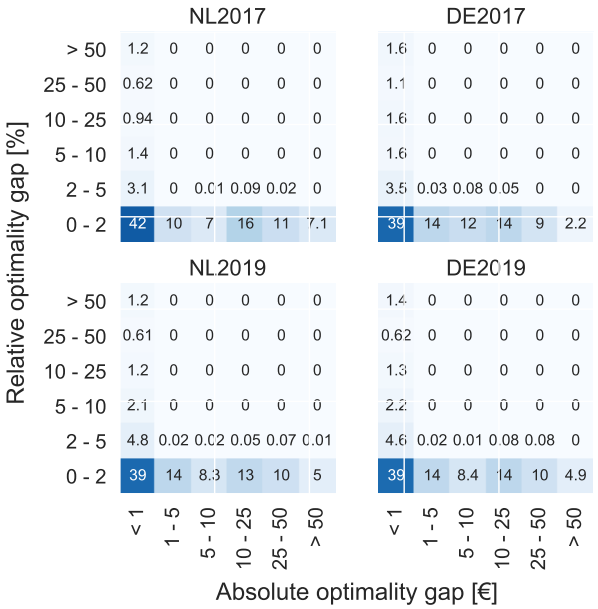

Figure 4: Percentage of occurrence of the combined termination conditions for the individual optimisation problems. Gurobi termination settings are at an absolute optimality gap of €1, or at a relative optimality gap of 2%.

The MPC implementation then solves the two optimisation problems (to minimise J_1 and J_2) in a receding horizon fashion, where the DAM participation (J_1) is optimised for every t_d time steps, and participation in the IDM is decided by solving J_2 every hour in a shrinking horizon fashion. The iterative two

phase optimisation problem, and the reference problem (J_3) can be stated as

$$\text{DAM planning phase: } \min_{(\cdot)} J_1(\cdot) + f_1(\cdot) \tag{21a}$$

$$\text{IDM trading phase: } \min_{(\cdot)} J_2(\cdot) + f_1(\cdot) \tag{21b}$$

$$\text{Futures market trading: } \min_{(\cdot)} J_3(\cdot) + f_1(\cdot) \tag{21c}$$

subject to:

$$h_{min} \leq h[t] \leq h_{max} + s[t] \tag{21d}$$

$$h[t] - (h[t-1] + \frac{\Delta t}{A} \cdot \ (Q_{in}[t-1] - Q_g[t-1] - Q_p[t-1])) \leq \delta_{wb} \tag{21e}$$

$$h[t] - (h[t-1] + \frac{\Delta t}{A} \cdot \ (Q_{in}[t-1] - Q_g[t-1] - Q_p[t-1])) \geq -\delta_{wb} \tag{21f}$$

$$h[t] - h_{ns}[t] - dH_{g,min} + (1 - z_g[t]) \cdot M_g \geq 0 \tag{21g}$$

$$h[t] - h_{ns}[t] - dH_{g,min} - z_g[t] \cdot M_g \leq 0 \tag{21h}$$

$$Q_g[t] \leq (a_g \cdot (h[t] - h_{ns}[t]) + b_g[t]) \cdot z_g[t] \tag{21i}$$

$$h_{ns}[t] - h[t] - dH_{p,min} + (1 - z_p[t]) \cdot M_p \geq 0 \tag{21j}$$

$$h_{ns}[t] - h[t] - dH_{p,min} - z_p[t] \cdot M_p \leq 0 \tag{21k}$$

$$Q_p[t] \leq (a_g[i] \cdot (h_{ns}[t] - h[t]) + b_p[i]) \cdot z_p[t] \text{ for } i \in (1,2,3) \tag{21l}$$

$$dH^2[t] = (h_{ns}[t] - h[t])^2 \tag{21m}$$

$$z_g \in (0,1) \tag{21n}$$

$$z_p \in (0,1) \tag{21o}$$

with

$$\begin{aligned} P[t] := a_p \cdot \ Q_p[t]^2 + b_p \cdot \ dH^2[t] \cdot \ Q_p[t] \\ + c_p \cdot \ Q_p[t] \cdot \ dH_p[t], \end{aligned} \tag{21p}$$

$$dH_p[t] := h_{ns}[t-1] - h[t-1] - dh_w[t-1] \tag{21q}$$

and the decision variables h, Q_g, Q_p stand for, respectively, the water level of the NZK, gate discharge and pump discharge. The slack variable s stands for the upper bound relaxation for water level constraints. The variables Q_{in} stand for the discharge flowing into the NZK-ARK system. Constants h_{min}, h_{max}, Δt, A, δ_{wb}, a_g, b_g, d_p, e_p, f_p, $dH_{g,min}$ and $dH_{p,min}$ stand for minimum and maximum water level allowed in the NZK-ARK, timestep size, storage area of the NZK-ARK, relaxation of the water balance constraint, fitted parameters for gate and pump discharge approximates and minimum water level difference needed for gate and pump discharge. Variables z_g and z_p are binary variables indicating gate- and pump-discharge possibilities through big-M constraints on the water level difference between the canal and the North Sea. The additional objective function terms $f_1(\cdot)$ (Equation (9)) is a linear penalty function on upper bound violations of the water level.

4. Results & Discussion

We simulate two 1-year periods, where costs are minimised using the multi-market strategy.We also simulate a reference scenario without DR, where energy use is minimised and energy costs are calculated using a monthly fixed futures market price. For the electricity markets, two years of real market data were used (2017, 2019). The hydrological forcings (incoming discharge and sea water level) of the system for the period (01-04-2017 - 31-03-2018) are used for both 2017 and 2019 simulations. The hydrological data was kept the same in order to be able to distinctly study the effect of a changing market and RES market

penetration on DR profitability. Actual DAM and IDM data is used, where for the IDM the ID3 IDM price was aggregated from the separate bids. For both the market data and the hydrological forcings, perfect forecasts are assumed. For the reference scenarios, the monthly-averaged futures market price is assumed. In the Dutch case, this is the ENDEX market while the Phelix-DE market price was used in the German case. The combination of minimising energy use while buying on the futures market is equivalent to the current strategy applied by RWS.

4.1. System dynamics

Figure 5 shows the actual and planned (at the time of the day ahead bid) fluxes (a, c), energy use and electricity prices (b, d) of water system using the multi-market strategy. The figure shows both the Dutch (left) and the German (right) market scenarios. The MPC tends to focus pumping on times where the water level difference with the North Sea is low when prices are positive, decreasing energy use. Both the gates and pumps don't violate the big-M constraint, forcing water to flow downwards and be pumped upwards only. In the depicted day, the North Sea is too high for the gates to be used. Negative prices can be seen in the German DAM, while they only occur in the Dutch IDM. Minimising cost when negative prices occur effectively leads to a maximisation of energy use. In the Dutch market, the MPC decides to sell energy bought for October 28th on the IDM for advantageous prices, and buys extra energy for October 29th for negative prices, counteracting a positive imbalance on the grid. On the German market, the MPC already maximises energy use on the DAM, restricting trade options on the IDM. However, some energy is sold on October 29th where positive prices occur on the IDM, counteracting a negative imbalance on the grid.

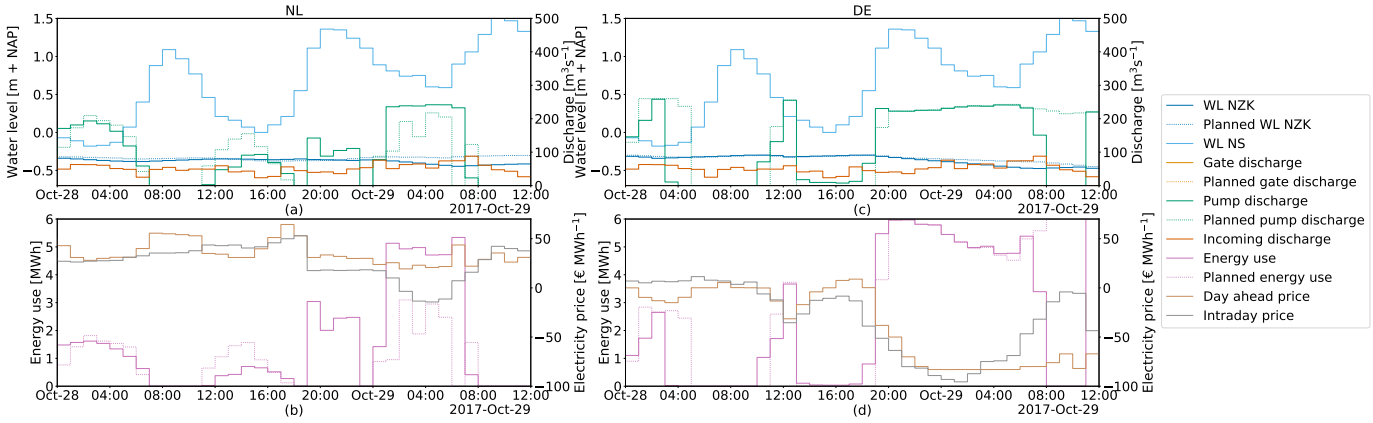

Figure 5: Optimised fluxes of the NZK-ARK (a, c), pump energy use and energy prices (b, d) for the Dutch market (left) and the German market (right). Thin and dashed lines show the planned course of action and the resulting water level at the time of day ahead market closing. Filled and thicker lines show the actual actions performed and the resulting water level after intraday trading.

4.2. Evaluation of DR profitability

The summarised performance of different scenarios can be seen in Table 2. It shows the relative costs of the proposed multi-market strategy compared to the reference futures market strategy. The relative energy use, the relative CO_2 emission, the average price of the used energy, the average CI of the used energy, and the percentage of energy that was used for negative energy prices are shown in the picture.

In both markets, optimising costs over the DAM and IDM leads to a significant cost decrease. In the German market the difference between spot and futures market participation is the largest, which can be explained by the higher share of renewable energy generation. Inflexible supply can lead to higher price volatility [60], rewarding flexibility. Uncertainty in energy generation makes a guaranteed base-load more expensive. Inflexibility in energy use is penalised when there is a higher market penetration of renewable energy and a lack of storage solutions, leading to negative energy prices.

Also, the large difference in costs between the markets can be explained by the increased price on carbon emission allowance [61]. This price creates a larger price difference between renewable and fossil energy, explaining the relatively low spot market prices in Germany compared to the futures market prices. Renewable energy makes up a higher share of the spot markets due to their unpredictable nature. This makes the increased carbon emission price mostly noticeable in the futures market, where base-load contracts can be supplied through the use of fossil sources. If both futures (i.e. Endex, Phelix-De) and spot markets (i.e. DAM, IDM) have a low penetration of renewable energy, like in the Dutch scenario, the spot market would experience the same price increase as the futures market.

In both the Dutch and German scenario, energy use is higher for the spot market scenarios than in the reference scenarios (where energy use is minimised), explaining the increase in carbon emission. The carbon emission does increase more slowly than the energy use, indicating a lower average CI of the used energy. The average price and CI of the used energy can be seen in Table 2, in both markets the average price of the used energy is lower for the spot market scenarios. The increase in energy use does not lead to an increase in costs. In the German case, the average price for the spot market scenarios is about a third of the average price for the reference scenarios. Also, a significant percentage of energy was used for negative prices, causing the MPC problem to maximise energy use. This explains the low average price, high cost savings, and high amount of extra energy use.

Even though the average price of the energy differs significantly between the futures and spot market scenarios, the average CI of the used energy is relatively similar. This shows that the base-level of the CI of the energy is not low enough to make up for the extra amount of energy being used. This holds for both the Dutch and the German markets. However, the average CI of the used energy is somewhat lower for the spot market scenarios, which can be explained by the correlation between CI and energy price shown in Figure 1c. In the German 2019 scenario, a 29% increase in energy use leads to a 5% CO_2 emission increase. This indicates that Germany is nearing a point where an increase in energy use would not lead to increased CO_2 emissions. Something that can possibly already be realised by limiting the energy use maximisation when negative prices occur, even though it's optimal for balancing the markets.

The relative cost differences show the influence of a higher futures market price on the potential cost savings through DR. Higher uncertainty in generation due to renewables make futures prices carry more risk-premiums, rewarding flexibility on the spot market while penalising inflexibility on baseload contracts.

Country	Year	Rel. costs	Rel. energy use	Rel. CO_2	Average energy price		Average CI		% of energy volume
					Spot	Futures	Spot	Futures	used with negative prices
NL	2017	0.90	1.07	1.05	31.81	37.60	421.22	428.84	0.00
	2019	0.84	1.29	1.16	30.94	47.31	271.59	301.51	0.92
DE	2017	0.44	1.32	1.15	11.93	35.44	319.52	365.43	11.44
	2019	0.50	1.29	1.05	17.67	45.43	222.10	273.41	14.25

Table 2: Relative profitability of DR over spot markets compared to futures market participation with fixed monthly prices. The rows show four scenarios of applying the multi-market MPC in DE and NL, using market data from two different years. The profitability of the multi-market strategy is divided by the profitability of the reference strategy without DR.

4.3. aFRR potential analysis

To investigate the potential for pumping station IJmuiden to be active on the aFRR market, we perform an analysis on the previous results where the pumping station is active on the DAM and IDM. The simulation data was used to determine if and when there was room within the constraints to realise a larger pump discharge. We assume the upper limit on the possible discharge to be the amount of water flowing into the system while being constrained by the Q-h curve of the pumping station, i.e. the added pumped volume would never lower the water level in the system. This ensures that water level constraints would not be violated by the additional use of the pumps, leading to a conservative estimate of extra pump capabilities. The extra room for pump use is translated into the amount of energy corresponding to this combination

of maximum discharge and pump height. The energy already bought on the DAM and IDM is subtracted from this amount.

The resulting data is used for two different analyses. In the first analysis, all DR events resulting in extra power consumption of more than 1 MW are selected to analyse aFRR potential during individual market participation (i.e. in the absence of an aggregator). In the second analysis, all DR events are selected to analyse aFFR potential when cooperating with an aggregator, thus allowing for small bids to be placed. In both cases, we selected the periods where downward activation in the aFRR market occurred simultaneously with a negative downward activation price. This allows us to calculate the maximum additional amount of energy that could have been profitably used for grid balancing purposes per timestep.

Table 3 shows the summary of results for the aFRR potential analysis. The results show that the aFRR market has the potential to compensate a part of the energy cost for pumping station IJmuiden. Although cost savings seem small, this analysis doesn't take the selling of energy due to the extra pumping into account. Besides that, the maximum amount of pumping for aFRR purposes was constrained to keep the water level equal, making the analysis a conservative estimate of the actual economic potential of participation in the aFRR. The results show that partnering with an aggregator could allow for substantial extra cost savings and regulating volume compared to participating on the market as a single bidder. The supplied downward regulating volume decreased from 2017 to 2019 in both the Dutch and German market scenario's. This indicates that the IDM is capable of supplying the necessary extra regulating volume due to renewable energy generation. The IDM is more accessible to BRPs, and carries relatively lower risk of disadvantageous prices due to the possibility to trade before delivery.

Country	Year	aFRR cost savings [%]		Downward regulating volume [MWh]	
		Individual	Aggregated	Individual	Aggregated
NL	2017	7.68	12.65	150.61	234.07
	2019	3.84	5.23	75.59	103.26
DE	2017	18.60	27.85	485.90	773.61
	2019	12.33	20.70	216.36	369.12

Table 3: Summarised results of aFRR market economic potential analysis: downward regulating volume and relative cost savings for scenarios with individual and aggregated market participation.

5. Conclusion

In this manuscript, we propose an economic two-stage MPC scheme to enable a large flood defense pumping station to participate in DR services. We explore how participating on the DAM gives more certainty of supply and costs while the IDM allows for short-notice trading, to make up for or exploit unforeseen events or dealing with uncertainties in the state of the open canal system. Therefore, a multi-market strategy is proposed, where pumping is scheduled a day ahead by buying energy on the DAM and then adjusted in a receding horizon fashion (every hour) when energy prices of the IDM are rewarding. We show that a larger profit can be realised for the pumping station when energy prices are more volatile, which can be expected to accompany a higher RES market penetration.

To demonstrate this, we explore the difference between the German and Dutch market scenarios, whose grids have a significantly different energy mix. We show that the proposed MPC is able to counteract both positive and negative imbalances on the grid through price-based DR. We also explore the effect of temporal market changes by using both 2017 and 2019 market data. A 46% and 50% cost decrease was found in the German market scenarios for the years 2017 and 2019 respectively, compared to the reference scenario. Negative energy prices on the German market were found to result in increased energy use and CO_2 emissions. The Dutch market scenario shows a 10% and 16% cost decrease in 2017 and 2019, respectively. The difference in potential cost saving shows that the German market rewards flexibility more than the Dutch market. We have shown that CO_2 savings are not yet present or well quantifiable in both German and Dutch cases.

The efficiency of pumping is time-dependent due to tides, resulting in an increased energy use when shifting pumping schedules for DR while the CI of the grid does not decrease enough for CO_2 emission savings to be present. Besides that, negative energy prices can lead to a significant increase in energy use. Although this is optimal from a market-perspective, it might not be preferred by the stakeholders. Also, generation by source time series are incorrect in the ENTSO-E transparancy platform, requiring us to estimate the CI time series through renewable energy production, observed load and reported CI estimates.

We show that participating in the aFRR market has economic potential, resulting in cost savings of up to 28% in the aggregated German scenario in 2017 based on our conservative analysis. Receiving a warning signal 15-minutes before activation makes the market feasible for the pumping station to be participate in. The analysis shows that aggregating participants, allowing them to circumvent the 1 MW minimum-bid constraint through pooling, results in higher participation and lower costs. In both German and Dutch markets, the aFRR economic potential decreased from 2017 to 2019. The supplied downward regulating volume decreased as well, indicating that the IDM could be supplying the extra balancing services required for renewable energy.

To conclude, we have shown that the economic potential for DR applied to open water systems is significant. However, it would be interesting to quantify the impact of uncertainty in system state, hydrological forcings (e.g. incoming discharge and sea water level) and energy prices, which are not considered in this manuscript. It is also known that variable speed pumps and more efficient configurations of more smaller pumps, in comparison to a single large pump, can expand the envelope for participation in DR [14]. Therefore, cost benefit analysis for the upgrading of the pumping station should be evaluated also explicitly considering performance in DR.

References

[1] International Energy Agency, Renewables 2017: Analysis and forecast to 2022, Tech. rep., International Energy Agency (IEA) (2017).

[2] Ministry of Economic Affairs and Climate Policy, Climate policy, accessed: 2019-05-28 (2019).
URL https://www.government.nl/topics/climate-change/climate-policy

[3] European Commission, 2050 low-carbon economy roadmap, Tech. rep., European Commission (2016).
URL https://ec.europa.eu/clima/policies/strategies/2050_en

[4] A. R. Jordehi, Optimisation of demand response in electric power systems, a review, Renewable and Sustainable Energy Reviews 103 (July 2018) (2019) 308–319. doi:10.1016/j.rser.2018.12.054.
URL https://doi.org/10.1016/j.rser.2018.12.054

[5] Liander, Liander wil flexibiliteitsmarkt starten in Nijmegen-Noord (2017).
URL https://www.alliander.com/nl/media/nieuws/liander-wil-flexibliteitsmarkt-starten-nijmegen-noord

[6] Fraunhofer Institute for solar energy systems ISE, Net public electricity generation in Germany in 2018, Tech. rep., Fraunhofer Institute for solar energy systems ISE (2019).
URL https://www.ise.fraunhofer.de/content/dam/ise/en/documents/News/Stromerzeugung_2018_2_en.pdf

[7] Ministerie van Economische Zaken, Energierapport: transitie naar duurzaam, Tech. rep., Ministerie van Economische Zaken (2016).
URL https://www.rijksoverheid.nl/binaries/rijksoverheid/documenten/rapporten/2016/01/18/energierapport-transitie-naar-duurzaam/energierapport-transitie-naar-duurzaam.pdf

[8] European Commission, Demand response in EU member states, Tech. rep., European Commission (2016).
URL http://publications.jrc.ec.europa.eu/repository/bitstream/JRC101191/ldna27998enn.pdf

[9] L. Raso, D. Schwanenberg, N. C. van de Giesen, P. J. van Overloop, Short-term optimal operation of water systems using ensemble forecasts, Advances in Water Resources 71 (2014) 200–208. doi:10.1016/j.advwatres.2014.06.009.
URL http://dx.doi.org/10.1016/j.advwatres.2014.06.009

[10] X. Tian, P. J. van Overloop, R. R. Negenborn, N. van de Giesen, Operational flood control of a low-lying delta system using large time step Model Predictive Control, Advances in Water Resources 75 (2015) 1–13. doi:10.1016/j.advwatres.2014.10.010.
URL http://dx.doi.org/10.1016/j.advwatres.2014.10.010

[11] X. Tian, Model Predictive Control for Operational Water Management: A Case Study of the Dutch Water System, 2015. doi:10.4233/uuid:aded9b65-677d-42bc-af93-969199aa1f77.

[12] X. Tian, R. R. Negenborn, P. J. van Overloop, J. María Maestre, A. Sadowska, N. van de Giesen, Efficient multi-scenario Model Predictive Control for water resources management with ensemble streamflow forecasts, Advances in Water Resources 109 (2017) 58–68. doi:10.1016/j.advwatres.2017.08.015.
URL https://doi.org/10.1016/j.advwatres.2017.08.015

[13] E. Nederkoorn, J. Schuurmans, J. Grispen, W. Schuurmans, Continuous nonlinear model predictive control of a hybrid water system, Journal of Hydroinformatics 15 (2) (2013) 246–257. doi:10.2166/hydro.2012.168.

[14] R. Menke, E. Abraham, P. Parpas, I. Stoianov, Extending the Envelope of Demand Response Provision though Variable Speed Pumps, Procedia Engineering 186 (2017) 584–591. doi:10.1016/j.proeng.2017.03.274.
URL http://dx.doi.org/10.1016/j.proeng.2017.03.274

[15] I. Pothof, K.-J. van Heeringen, T. Piovesan, T. Vreeken, L. Loverdou, J. Talsma, H. Kuipers, B. van Esch, E. al., Slim malen, Tech. rep., STOWA (2019).
URL https://www.stowa.nl/sites/default/files/assets/PUBLICATIES/Publicaties2019/STOWA2019-27slimmalendefdefversie.pdf

[16] TenneT TSO B.V., aFRR pilot end report, Tech. rep., TenneT (2021).
URL https://www.tennet.eu/fileadmin/user_upload/SO_NL/aFRR_pilot_end_report.pdf

[17] G. Strbac, Demand side management: Benefits and challenges, Energy policy 36 (12) (2008) 4419–4426.

[18] K. Saxena, R. Bhakar, Impact of LRIC pricing and demand response on generation and transmission expansion planning, IET Generation, Transmission and Distribution 13 (5) (2019) 679–685. doi:10.1049/iet-gtd.2018.5328.

[19] J. Contreras, M. Asensio, P. M. de Quevedo, G. Muñoz-Delgado, S. Montoya-Bueno, Joint RES and Distribution Network Expansion Planning under a Demand Response Framework, Academic Press, 2016.

[20] J. G. Kirkerud, N. O. Nagel, T. F. Bolkesjø, The role of demand response in the future renewable northern European energy system, Energy 235 (2021) 121336. doi:10.1016/j.energy.2021.121336.
URL https://doi.org/10.1016/j.energy.2021.121336

[21] C. Mkireb, A. Dembélé, A. Jouglet, T. Denoeux, Robust Optimization of Demand Response Power Bids for Drinking Water Systems, Applied Energy 238 (2019) 1036–1047. doi:10.1016/j.apenergy.2019.01.124.
URL https://doi.org/10.1016/j.apenergy.2019.01.124

[22] R. Menke, E. Abraham, P. Parpas, I. Stoianov, Demonstrating demand response from water distribution system through pump scheduling, Applied Energy 170 (2016) 377–387. doi:10.1016/j.apenergy.2016.02.136.
URL http://dx.doi.org/10.1016/j.apenergy.2016.02.136

[23] R. Menke, K. Kadehjian, E. Abraham, I. Stoianov, Investigating trade-offs between the operating cost and green house gas emissions from water distribution systems, Sustainable Energy Technologies and Assessments 21 (2017) 13–22. doi:10.1016/j.seta.2017.03.002.
URL http://dx.doi.org/10.1016/j.seta.2017.03.002

[24] C. Mkireb, A. Dembele, A. Jouglet, T. Denoeux, A linear programming approach to optimize demand response for water systems under water demand uncertainties, 2018 International Conference on Smart Grid and Clean Energy Technologies, ICSGCE 2018 (2018) 206–211doi:10.1109/ICSGCE.2018.8556696.

[25] K. Oikonomou, M. Parvania, R. Khatami, Optimal Demand Response Scheduling for Water Distribution Systems, IEEE Transactions on Industrial Informatics 14 (11).
URL https://ieeexplore.ieee.org/stamp/stamp.jsp?tp={&}arnumber=8279561

[26] G. Bianchini, M. Casini, A. Vicino, D. Zarrilli, Demand-response in building heating systems: A Model Predictive Control approach, Applied Energy 168 (2016) 159–170. doi:10.1016/j.apenergy.2016.01.088.
URL http://dx.doi.org/10.1016/j.apenergy.2016.01.088

[27] F. A. Qureshi, T. T. Gorecki, C. N. Jones, Model predictive control for market-based demand response participation, Vol. 19, IFAC, 2014. doi:10.3182/20140824-6-ZA-1003.02395.
URL http://dx.doi.org/10.3182/20140824-6-ZA-1003.02395

[28] R. E. Hedegaard, T. H. Pedersen, S. Petersen, Multi-market demand response using economic model predictive control of space heating in residential buildings, Energy and Buildings 150 (2017) 253–261. doi:10.1016/j.enbuild.2017.05.059.
URL http://dx.doi.org/10.1016/j.enbuild.2017.05.059

[29] A. Y. Yoon, Y. J. Kim, S. I. Moon, Optimal Retail Pricing for Demand Response of HVAC Systems in Commercial Buildings Considering Distribution Network Voltages, IEEE Transactions on Smart Grid 10 (5) (2018) 5492–5505. doi:10.1109/TSG.2018.2883701.

[30] D. Schwabeneder, C. Corinaldesi, G. Lettner, H. Auer, Business cases of aggregated flexibilities in multiple electricity markets in a European market design, Energy Conversion and Management 230 (August 2020) (2021) 113783. doi:10.1016/j.enconman.2020.113783.
URL https://doi.org/10.1016/j.enconman.2020.113783

[31] M. McPherson, B. Stoll, Demand response for variable renewable energy integration: A proposed approach and its impacts, Energy 197 (2020) 117205. doi:10.1016/j.energy.2020.117205.
URL https://doi.org/10.1016/j.energy.2020.117205

[32] D. Zhang, N. Shah, L. G. Papageorgiou, Efficient energy consumption and operation management in a smart building with microgrid, Energy Conversion and Management 74 (2013) 209–222. doi:10.1016/j.enconman.2013.04.038.
URL http://dx.doi.org/10.1016/j.enconman.2013.04.038

[33] A. Leon-Garcia, Price Prediction in Real-Time Electricity, IEEE Transactions on Smart Grid 1 (2) (2010) 120–133.
URL http://ieeexplore.ieee.org/lpdocs/epic03/wrapper.htm?arnumber=5540263

[34] D. Setlhaolo, X. Xia, J. Zhang, Optimal scheduling of household appliances for demand response, Electric Power Systems Research 116 (2014) 24–28. doi:10.1016/j.epsr.2014.04.012.
URL http://dx.doi.org/10.1016/j.epsr.2014.04.012

[35] N. I. Nwulu, X. Xia, Optimal dispatch for a microgrid incorporating renewables and demand response, Renewable Energy 101 (2017) 16–28. doi:10.1016/j.renene.2016.08.026.
URL http://dx.doi.org/10.1016/j.renene.2016.08.026

[36] G. Litjens, E. Worrell, W. van Sark, Economic benefits of combining self-consumption enhancement with frequency restoration reserves provision by photovoltaic-battery systems, Applied Energy 223 (2018) 172 – 187. doi:https://doi.

org/10.1016/j.apenergy.2018.04.018.
URL http://www.sciencedirect.com/science/article/pii/S0306261918305622
[37] L. R. Rodríguez, M. Brennenstuhl, M. Yadack, P. Boch, U. Eicker, Heuristic optimization of clusters of heat pumps: A simulation and case study of residential frequency reserve, Applied Energy 233-234 (2019) 943 – 958. doi:https://doi.org/10.1016/j.apenergy.2018.09.103.
URL http://www.sciencedirect.com/science/article/pii/S0306261918314247
[38] O. Kilkki, I. Seilonen, K. Zenger, V. Vyatkin, Optimizing residential heating and energy storage flexibility for frequency reserves, International Journal of Electrical Power & Energy Systems 100 (2018) 540 – 549. doi:https://doi.org/10.1016/j.ijepes.2018.02.047.
URL http://www.sciencedirect.com/science/article/pii/S0142061517322615
[39] P. Li, Z. Wang, J. Wang, W. Yang, T. Guo, Y. Yin, Two-stage optimal operation of integrated energy system considering multiple uncertainties and integrated demand response, Energy 225 (2021) 120256. doi:10.1016/j.energy.2021.120256.
URL https://doi.org/10.1016/j.energy.2021.120256
[40] J. De Jong, A. Hassel, J. Jansen, C. Egenhofer, Z. Xu, Improving the Market for Flexibility in the Electricity Sector, Tech. rep., Centre for European Policy Studies (2017).
URL http://aei.pitt.edu/92294/1/CEPS{_}TFR{_}Flexibility{_}Electricity{_}Markets.pdf
[41] TenneT, Annual market update 2017, accessed: 2019-12-19 (2017).
URL https://www.tennet.eu/fileadmin/user_upload/Company/Publications/Technical_Publications/Dutch/2017_TenneT_Market_Review.pdf
[42] P. Bertoldi, P. Zancanella, B. Boza-Kiss, Demand Response status in EU Member States, Tech. rep., European Commission (2016). doi:10.2790/962868.
URL https://iet.jrc.ec.europa.eu/energyefficiency/sites/energyefficiency/files/publications/demand{_}response{_}status{_}in{_}eu28{_}member{_}states-online.pdf
[43] S. Pfenninger, I. Staffell, Long-term patterns of European PV output using 30 years of validated hourly reanalysis and satellite data, Energy 114 (2016) 1251–1265. doi:10.1016/j.energy.2016.08.060.
URL http://dx.doi.org/10.1016/j.energy.2016.08.060
[44] I. Staffell, S. Pfenninger, Using bias-corrected reanalysis to simulate current and future wind power output, Energy 114 (2016) 1224–1239. doi:10.1016/j.energy.2016.08.068.
URL http://dx.doi.org/10.1016/j.energy.2016.08.068
[45] Centraal Bureau van de Statistiek, Statline - elektriciteit en warmte; producie en inzet naar energiedrager, accessed: 2019-07-17 (2019).
URL https://opendata.cbs.nl/statline/#/CBS/nl/dataset/80030ned/table?fromstatweb
[46] Fraunhofer-Institut für Solar Energiesysteme ISE, Energy charts (2021).
URL https://energy-charts.info/?l=de&c=DE
[47] A. E. E.V., Ausdruck strerz abgabe dez2020 anteile (2020).
URL https://ag-energiebilanzen.de/index.php?article_id=29&fileName=ausdruck_strerz_abgabe_dez2020_anteile_.xlsx
[48] M. Pehl, A. Arvesen, F. Humpenöder, A. Popp, E. Hertwich, G. Luderer, Understanding future emissions from low-carbon power systems by integration of life-cycle assessment and integrated energy modelling, Nature Energy 2 (2017) 939–945. doi:10.1038/s41560-017-0032-9.
URL https://doi.org/10.1038/s41560-017-0032-9
[49] A. Bonou, A. Laurent, S. I. Olsen, Life cycle assessment of onshore and offshore wind energy-from theory to application, Applied Energy 180 (2016) 327–337. doi:10.1016/j.apenergy.2016.07.058.
URL http://dx.doi.org/10.1016/j.apenergy.2016.07.058
[50] E. E. Agency, Greenhouse gas emission intensity of electricity generation (2020).
URL https://www.eea.europa.eu/data-and-maps/daviz/co2-emission-intensity-8/
[51] ENTSO-E, Entso-e transparancy platform (2018).
URL https://transparency.entsoe.eu/
[52] H. Janssen, Effect selectieve onttrekking IJmuiden op waterbeheer, Tech. rep., Rijkswaterstaat (2017).
URL https://www.platformparticipatie.nl/binaries/Effect%20selectieve%20onttrekking%20IJmuiden%20op%20waterbeheer_tcm117-377563.pdf
[53] R. van Weissenbruch, Onderzoek energieverbruik gemaal IJmuiden, Master's thesis, TU Delft (2003).
[54] A. Goedbloed, Kwaliteitsanalyse beslissings ondersteunend systeem Noordzeekanaal/Amsterdam-Rijnkanaal, Tech. rep., Delft University of Technology (2006).
URL https://datachallenge.nl/files/Aanvoermodule%20RWS%20-%20Rapport%20kwaliteitsanalyse_BOS_NZKARK%20Goedbloed.pdf
[55] HKV, Doorontwikkeling DEZY 2.0, Tech. rep., HKV (2016).
[56] B. K. C. Geerse, Probabilistisch model frequentielijnen ijsselmeergebied: Hoofdrapport van model dezy, Tech. rep., HKV (2015).
[57] J. M. Maestre, L. Raso, P. J. Van Overloop, B. De Schutter, Distributed tree-based model predictive control on a drainage water system, Journal of Hydroinformatics 15 (2) (2013) 335–347. doi:10.2166/hydro.2012.125.
[58] R. Menke, E. Abraham, P. Parpas, I. Stoianov, Exploring optimal pump scheduling in water distribution networks with branch and bound methods, Water Resources Management 30 (14) (2016) 5333–5349.
[59] Gurobi Optimization, LLC, Gurobi optimizer reference manual (2018).
URL http://www.gurobi.com

[60] S. Mosquera-López, A. Nursimulu, Drivers of electricity price dynamics: Comparative analysis of spot and futures markets, Energy Policy 126 (October 2018) (2019) 76–87. doi:10.1016/j.enpol.2018.11.020.
URL https://doi.org/10.1016/j.enpol.2018.11.020

[61] TenneT, Annual market update 2018, accessed: 2019-07-19 (2018).
URL https://www.tennet.eu/fileadmin/user_upload/Company/Publications/Technical_Publications/Dutch/Annual_Market_Update_2018_-_Final.pdf